Molecular Crystals and Liquid Crystals

Publication details, including instructions for authors and subscription information:
http://www.tandfonline.com/loi/gmcl20

Hybrid Polymer Nanoassemblies Consisting of Polymer Nanosheets and Metal Nanoparticle Arrays

Masaya Mitsuishi [a], Miki Ishifuji [a], Hiroshi Endo [a], Hiroyuki Tanaka [a] & Tokuji Miyashita [a]

[a] Institute of Multidisciplinary Research for Advanced Materials (IMRAM), Tohoku University, Katahira, Aoba-ku, Japan

Version of record first published: 22 Sep 2010

To cite this article: Masaya Mitsuishi, Miki Ishifuji, Hiroshi Endo, Hiroyuki Tanaka & Tokuji Miyashita (2007): Hybrid Polymer Nanoassemblies Consisting of Polymer Nanosheets and Metal Nanoparticle Arrays, Molecular Crystals and Liquid Crystals, 471:1, 11-19

To link to this article: http://dx.doi.org/10.1080/15421400701544448

Mol. Cryst. Liq. Cryst., Vol. 471, pp. 11–19, 2007

ISSN: 1542-1406 print/1563-5287 online
DOI: 10.1080/15421400701544448

Taylor & Francis
Taylor & Francis Group

Hybrid Polymer Nanoassemblies Consisting of Polymer Nanosheets and Metal Nanoparticle Arrays

Masaya Mitsuishi
Miki Ishifuji
Hiroshi Endo
Hiroyuki Tanaka
Tokuji Miyashita
Institute of Multidisciplinary Research for Advanced Materials (IMRAM), Tohoku University, Katahira, Aoba-ku, Japan

The article describes hybrid polymer nanoassemblies consisting of polymer nanosheets and metal nanoparticle arrays. Ultrathin polymer Langmuir-Blodgett films were utilized to assemble metal nanoparticles, to make free-standing hybrid polymer nanosheets, to examine the possibility of hybrid polymer nanoassemblies as luminescence sensor application, and to orient nonlinear optical (NLO) active molecules. Assembling nanomaterials such as nanoparticle and organic functional molecules through bottom-up approach make it possible to strengthen free-standing nanofilm stability, enhance luminescence from luminescent molecules and second harmonic light from NLO molecules under the influence of localized surface plasmon.

Keywords: free-standing; LB film; metal nanoparticle; polymer; surface plasmon

1. INTRODUCTION

Recently, metal nanoparticle ordering has much attention, because it shows fascinating features such as quantum size effect, catalytic activity, and localized surface plasmon. We have investigated preparation of metal nanoparticle arrays with polymer nanosheets through electrostatic interaction [1]. Polymer nanosheets [2] consist of cationic

The work is supported by a Grant-in Aid for Scientific Research ((S) No. 17105006), Young Scientists ((A), No. 18685027), and Priority Areas (No. 417).

Address correspondence to Masaya Mitsuishi, Institute of Multidisciplinary Research for Advanced Materials (IMRAM), Tohoku University, 2-1-1 Katahira, Aoba-ku 980-8577, Japan. E-mail: masaya@tagen.tohoku.ac.jp

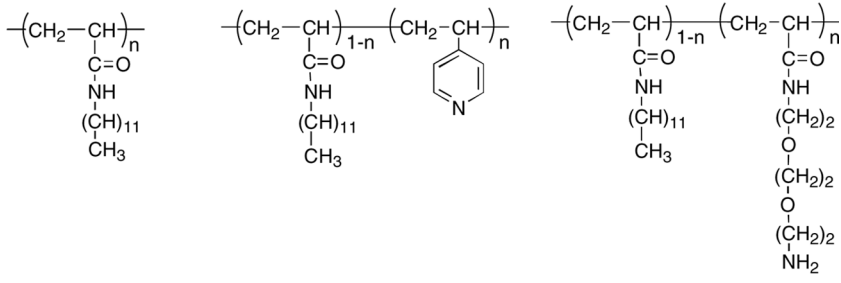

FIGURE 1 Chemical structure of polymer nanosheet (a) pDDA, (b) p(DDA/VPy), (c) p(DDA/DADOO).

comonomer and *N*-dodecylacrylamide capable of forming Langmuir-Blodgett films (Fig. 1). We assembled functional polymer nanosheets with metal nanoparticle monolayers to utilize localized surface plasmon as an excitation source. The hybrid polymer nanoassemblies give strong absorption bands in the visible light wavelength due to surface plasmon resonance coupling of metal nanoparticle arrays and are expected to open up possibility for opto/electric device application. For example, surface plasmon generated from silver nanoparticle array enhances luminescence of ruthenium complex and metallo-porphyrin complex [3]. Besides, nanoparticle arrays exhibit filler effects to strengthen the film stability [4]. In this article, we describe recent topics of hybrid polymer nanoassemblies based on polymer nanosheets: free-standing hybrid polymer nanosheets, optical sensor application of hybrid polymer nanoassemblies, and second harmonic generation from polymer nanosheets enhanced by coupled surface plasmon resonance.

1.1. Free-Standing Hybrid Polymer Nanosheets

The experimental outline of free-standing hybrid poltmer nanosheets is shown in Figure 2 [5]. We deposited 10-layer pDDA nanosheets and two-layer p(DDA/DADOO) nanosheets on a silicon wafer, Gold nanoparticles were immobilized on the film. The surface was covered with photo-cross-linkable polymer nanosheets (p(DDA/M), see Fig. 2). The substrate was irradiated with deep UV light and immersed in chloroform. The ultrathin film was removed from the surface. We tried to transfer the film on a copper TEM grid. The holes (85 μm diameter) of the TEM grid were successfully covered with the free-standing hybrid polymer nanosheets. It should be mentioned that it was difficult to peel off the film without gold nanoparticle layer in

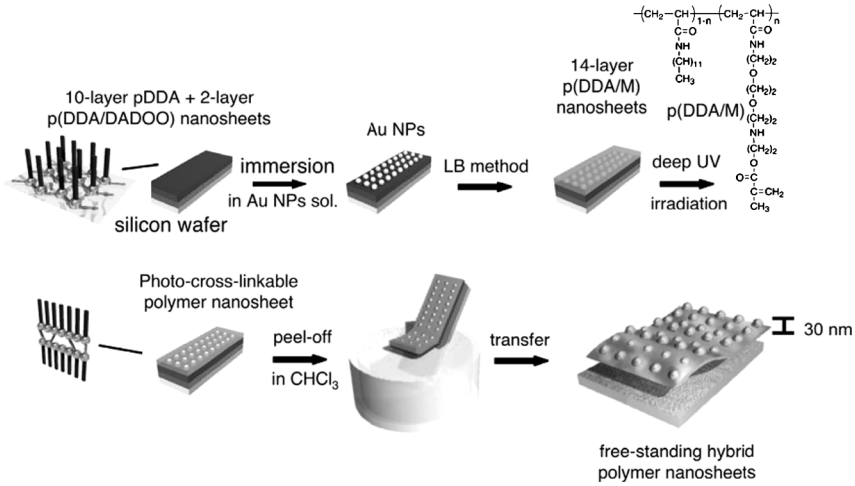

FIGURE 2 Schematics of preparation of free-standing hybrid polymer nanosheets.

this procedure. In other words, gold nanoparticles acts as "nano-filler." We succeeded in preparation of free-standing hybrid polymer nanosheets, which had large size (over 50 mm^2) and high durability (for several months). Figure 3 shows AFM images of hybrid free-standing polymer nanosheets. The film thickness was determined to

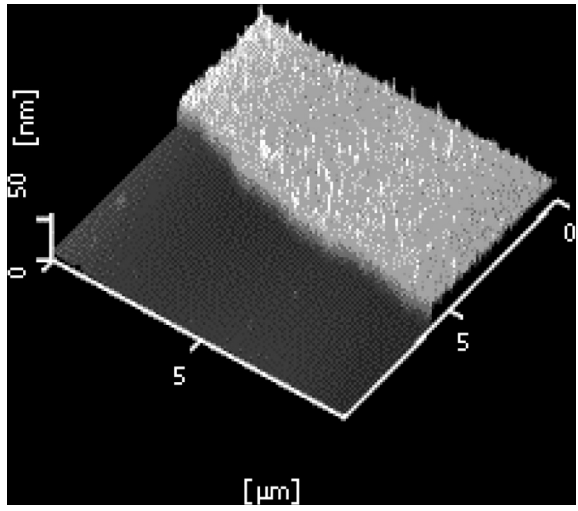

FIGURE 3 AFM image of free-standing hybrid polymer nanosheets.

be approximately 30 nm. This is the same as the diameter of gold nanoparticles mixed in the film. Assuming that the p(DDA/M) nanosheets take a fairly flat multilayer structure on the gold nanoparticle layer, the layer thickness is $2.0 \times 14 = 28\,(\mathrm{nm})$. Considering the free-standing film thickness (30 nm) and the surface coverage of gold nanoparticles (42%), the outermost layer can fill the gap between gold nanoparticles. After deep UV irradiation, the p(DDA/M) nanosheets undergo photo-cross-linking reaction and might take thermal relaxation, keeping the gold nanoparticles separated from each other. Consequently, the free-standing hybrid polymer nanosheet has uniform distribution of gold nanoparticles and smooth surface. These results indicate that gold nanoparticles make polymer nanosheets robust and easy to release from the solid supports.

1.2. Optical Sensor for Molecular Oxygen Based on Luminescence Quenching under Localized Surface Plasmon Excitation

Ruthenium complexes are well known luminescent molecules which have high quantum yield, long excited-state lifetime, and strong absorption in the blue-green spectral region. The luminescence is easily quenched by molecular oxygen. We have succeeded in incorporation of ruthenium complexes in polymer nanosheets and examined the possibility of the luminescent polymer nanosheets for oxygen sensor application [6]. The luminescent polymer nanosheet covers various surface smoothly, and enables the surface oxygen concentration to be detected as luminescence intensity change, The faster optical response is expected by using these ultrathin films, however, it seems to be difficult to gain the luminescence intensity to be required due to shortage of the amount of luminophores. To overcome this drawback, we tried to enhance the luminescence from ruthenium complexes incorporated in polymer nanosheets by utilizing localized surface plasmon electromagnetic field as an excitation source [7].

We prepared polymer nanosheets having ruthenium complexes ($\mathrm{Ru(dpphen)}_3^{2+}$) by polyion complex method [6]. The concentration of $\mathrm{Ru(dpphen)}_3^{2+}$ is adjustable by varying acrylic acid group content. Figure 4 shows luminescence spectra of p(DDA-Ru) nanosheets (four layers, excitation wavelength = 440 nm) as a function of oxygen concentration. Assembling silver nanoparticle (80 nmϕ) monolayer on the p(DDA-Ru) nanosheets (Fig. 4(b)), the four-fold luminescence intensity enhancement was achieved. Similar to the case of $\mathrm{Ru(bpy)}_3^{2+}$ [7], surface plasmon electromagnetic field generated around silver

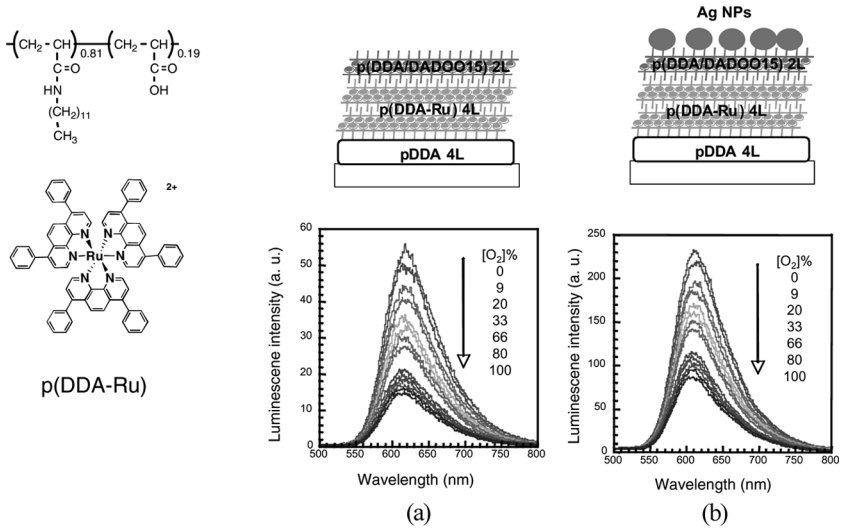

FIGURE 4 Chemical structure of p(DDA-Ru) and luminescence spectra of four-layer p(DDA-Ru) nanosheets as a function of oxygen concentration. The top of Figures 4(a) and 4(b) show the layer structure.

nanoparticle enhances excitation efficiency of $Ru(dpphen)_3^{2+}$ incorporated in p(DDA-Ru) nanosheets. Figure 5 shows Stern-Volmer relationship for p(DDA-Ru) nanosheets. Linear Stern-Volmer plots were obtained for both p(DDA-Ru) nanosheets and hybrid polymer nanoassemblies, indicating the uniform microenvironment around ruthenium complexes. The sensitivity of the hybrid polymer nanoassemblies decreases comparing with that of p(DDA-Ru) nanosheets alone. It should be mentioned that the sensitivity of p(DDA-Ru) nanosheets for oxygen concentration is lower than that of $Ru(dpphen)_3^{2+}$, probably due to the less accessibility of oxygen to $Ru(dpphen)_3^{2+}$ protected by long alkyl side chains [8]. The response for oxygen concentration was reversible and its time response was apparently 20 s, however, the response should be much faster because the change in oxygen concentration was a rate-determining process.

1.3. Second Harmonic Generation from Hybrid Polymer Nanoassemblies

We used disperse red 1 as an NLO active moiety (DR) and copolymerized with DDA through free radical copolymerization (p(DDA/DR)), $Mn = 2.80 \times 10^3$, $Mw/Mn = 1.58$, 18 mol% DR content) (Fig. 6). Homopolymer, pDDA was used as an inert layer. Alternate LB film

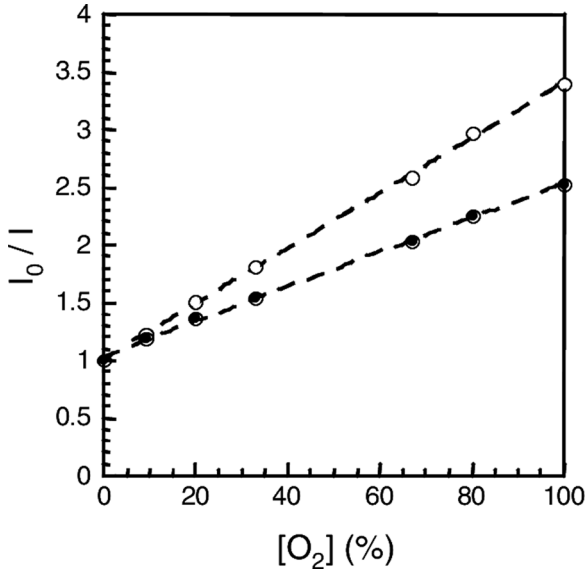

FIGURE 5 Stern-Volmer plots of p(DDA-Ru) nanosheets with Ag NPs (open circle) and without Ag NPs (filled circle).

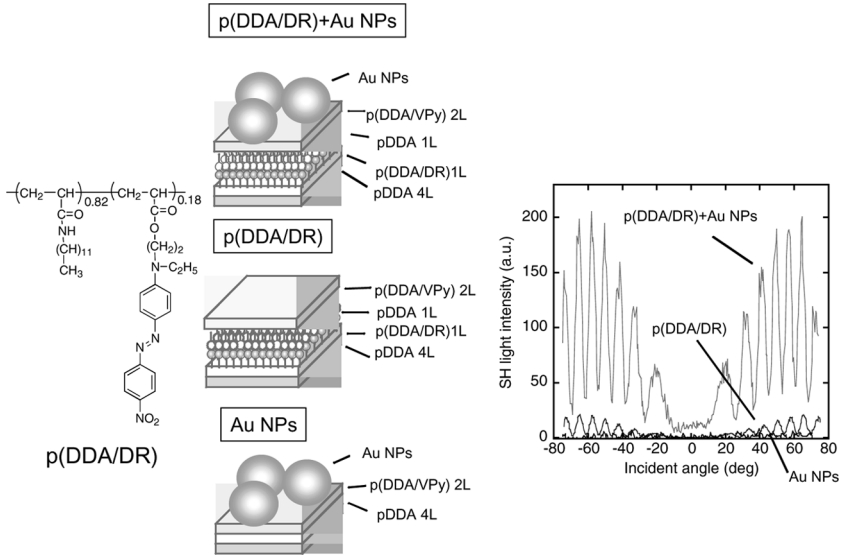

FIGURE 6 (left) Chemical structure of p(DDA/DR) (middle) layer structures of NLO active polymer nanosheet (right) SH fringe patterns of p(DDA/DR) nanosheets for respective layer structures.

deposition was carried out with an automatically controlled LB trough [9]. A glass substrate was rendered hydrophobic using octyltrichlorosilane. The surface was precoated with four-layer pDDA nanosheets to avoid surface effects. We constructed hetero-structured polymer nanosheets by transferring p(DDA/DR) (downstroke) and pDDA (upstroke) alternately at the surface pressure and temperature of 30.0 mN/m for pDDA, 15.0 mN/m for p(DDA/DR), and 20.0°C. Two-layer cationic polymer nanosheets, p(DDA/VPy) (Fig. 1) at 35 mN/m and 15.0°C, were deposited on the hetero-deposited polymer nanosheets. The substrate was immersed in a gold nanoparticle (30 nmϕ) aqueous solution.

Figure 6 shows the SH light interference pattern obtained from 1 bilayer film of p(DDA/DR) and pDDA coated on both sides of the glass substrates (Fig. 6, p(DDA/DR)). Dependence of the SH light intensity with respect to the incident angle shows a well-contrasted fringe pattern resulting from interference between the emitted SH light produced by the front and back layers. Interestingly, the SH light intensity is enhanced drastically under gold nanoparticle arrays (Fig. 6, p(DDA/DR) + Au NPs) [10]. The clear SH light interference pattern also indicates that the gold nanoparticle arrays are immobilized uniformly on the hetero-structured polymer nanosheets and thereby produce a monoparticle layer, engendering no aggregate formation that would affect the light coherence and scattering.

We measured UV-Vis absorption spectra of hybrid polymer nanoassemblies as a function of immersion time in gold nanoparticle aqueous solution. As the immersion time increased, the number of gold nanoparticles immobilized on the polymer ultrathin film surface increased. Nearer gold nanoparticles generate a coupled surface plasmon electromagnetic field, resulting in a red shift of the absorption band broadened to 1500 nm. Figure 7 shows the absorbance at 532 nm and 1064 nm and the SH light intensity of hybrid polymer nanoassemblies with different immersion times. Interestingly, no remarkable SH light intensity enhancement was observed below 8 h, and eight-fold enhancement was achieved at 12 h immersion time. The change in SH light intensity is closely coincident with that in absorbance at 1064 nm, though the absorbance at 532 nm increases monotonically. As the immersion time becomes greater than 6 h, the gold nanoparticles increase so that they interact electromagnetically with each other. The electromagnetic field enhancement at 1064 nm is attributable to the dipole-like coupled surface plasmon mode generated between adjacent gold nanoparticles. This is a plausible reason for the SH light intensity enhancement. It should be mentioned that no considerable SH light intensity was obtained from gold nanoparticle

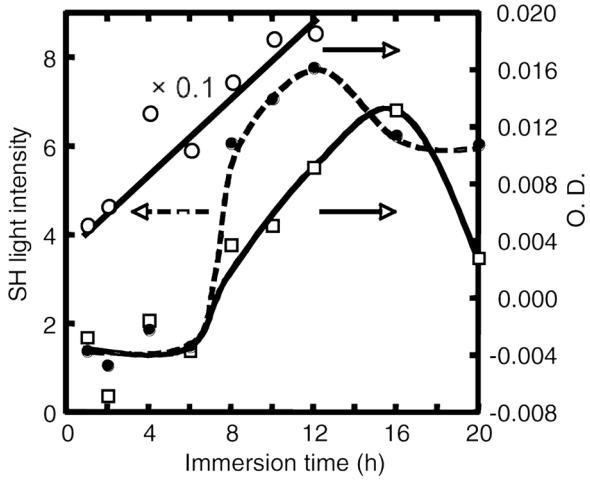

FIGURE 7 Plots of SH light intensity (filled circle), absorbance at 1064 nm (open rectangle) and 532 nm (open circle) as a function of immersion time.

arrays alone (Fig. 6, Au NPs). These results strongly imply that gold nanoparticle ordering for creating coupled surface plasmon electromagnetic field and hybridization of NLO active molecules with gold nanoparticle arrays at the nanometer scale are important for SH light intensity enhancement based on surface plasmon resonance.

2. CONCLUSION

We describe effective approach of hybrid polymer nanoassemblies for preparing self-standing ultrathin film, extending the luminescent ultrathin film to sensor application, and enhancing SH light intensity under coupled SPR. Due to its strong absorption at visible light region, it is possible to realize the free-standing film even its thickness corresponds to the nanoparticle diameter. To utilize localized surface plasmon effectively, it is important to assemble metal nanoparticle (Au and Ag) with photo/electro functional molecules at the nanometer precision, because surface plasmon is confined on the metal surface. In this sense, detailed investigation of luminescence or SHG properties of hybrid polymer nanoassemblies will provide deep understanding of localized surface plasmon coupled with functional molecules.

REFERENCES

[1] Tanaka, H., Mitsuishi, M., & Miyashita, T. (2003). *Langmuir*, *19*, 3103.
[2] Mitsuishi, M., Matsui, J., & Miyashita, T. (2006). *Polym. J.*, *38*, 877.

[3] (a) Lakowicz, J. R., Shen, Y., D'Auria, S., Malicka, J., Fang, J., Gryczynski, Z., & Gryczynski, I. (2002). *Anal. Biochem.*, *301*, 261; (b) Pan, S. & Rothberg, L. J. (2005). *J. Am. Chem. Soc.*, *127*, 6087.
[4] Mamedov, A. A. & Kotov, N. A. (2000). *Langmuir*, *16*, 5530.
[5] Endo, H., Kado, Y., Mitsuishi, M., & Miyashita, T. (2006). *Macromolecules*, *39*, 5559.
[6] Miyashita, T., Chen, J., Yuasa, M., & Mitsuishi, M. (1999). *Polym. J.*, *31*, 1121.
[7] Tanaka, H., Mitsuishi, M., & Miyashita, T. (2005). *Chem. Lett.*, *34*, 1246.
[8] Chu, B. W.-K. & Yam, V. W.-W. (2006). *Langmuir*, *22*, 7437.
[9] Ishifuji, M., Mitsuishi, M., & Miyashita, T. (2005). *Nonlinear Opt. Quantum Opt.*, *34*, 111.
[10] Ishifuji, M., Mitsuishi, M., & Miyashita, T. (2006). *Appl. Phys. Lett.*, *89*, 011903.